



# Volcanic ash from La Palma (Canary Islands, Spain) as Portland cement constituent

Miguel Angel Sanjuán<sup>a</sup>, Moisés Frías<sup>b,\*</sup>, Manuel Monasterio<sup>b</sup>,  
Rosario García-Giménez<sup>c</sup>, Raquel Vigil de la Villa<sup>c</sup>, Montse Álamo<sup>d</sup>

<sup>a</sup> Spanish Institute of Cement and its Applications (IECA), 28003, Madrid, Spain

<sup>b</sup> Eduardo Torroja Institute (IETcc-CSIC), C/ Serrano Galvache, 4, 28033, Madrid, Spain

<sup>c</sup> Department of Geology and Geochemistry, Faculty of Science, Geomaterials – associated unit (CSIC-UAM), Autonomous University of Madrid, 28049, Madrid, Spain

<sup>d</sup> Cementos Especiales de Las Islas, S.A. ("CEISA"), Arguineguín, Gran Canaria, Canary Islands, Spain

## ARTICLE INFO

### Keywords:

Volcanic ash  
Characterization  
Blended cements  
Physical-mechanical properties  
Climate change

## ABSTRACT

The last volcanic eruption on the island of La Palma (Spain) took place in 2021. Significant activity started in September of that year with the vigorous emission of volcanic gases and ash and lasted for three months. It is estimated that the Cumbre Vieja volcano emitted more than ten million cubic meters of ash comprising pyroclastic materials like those found in many parts of the world. Some of these volcanic ash deposits are untapped, despite their potential construction industry applications. Since the chemical composition and mineralogy of the ash depends on the type of magma from it originates, this paper characterizes this material and evaluates its suitability as a major constituent of Portland cement. This volcanic ash is rich in silica (45%) and alumina (15%), meaning it reacts with portlandite. The blended cements with up to 40% replacement content meet the standardized chemical, physical, and mechanical requirements and present good intrinsic durability values (resistivity and capillary absorption), making them viable for the manufacture of low-carbon-footprint eco-cements. This paper seeks to provide society with lasting technical, environmental, and social benefits through recovery of this ash.

## 1. Introduction

The southern part of the island of La Palma has suffered a series of volcanic eruptions over the years, with the hitherto most recent occurring in 1949 and 1971. Most of the lava flows and eruptions occurred on the western slope of the Cumbre Vieja volcano, the most active in the Canary Islands with eight eruptions between 1500 and 2020 [1,2]. The 2021 eruption at a location formerly called Hoya de Tajogaite (Fig. 1) was the most intense in terms of duration (it began on September 19 and ended on December 13, 2021 and remained active for 85 days) and area covered by lava flows (65 km<sup>2</sup>) [3]. Furthermore, the area affected by deposition of volcanic ash, such as tephra and lapilli, is even larger, although it is not clearly defined [4]. This ash was deposited across the island of La Palma and even reached the neighboring islands of El Hierro and Tenerife. To better understand the ash dispersion mechanisms, the volcanic eruption has been studied by the State Meteorological Agency of Spain (AEMET) to learn more about the emitted ash and its microphysical properties [5]. Additionally, it is important to note that this volcanic eruption was the most destructive experienced in

\* Corresponding author.

E-mail addresses: [masanjuan@ieca.es](mailto:masanjuan@ieca.es) (M.A. Sanjuán), [mfrias@ietcc.csic.es](mailto:mfrias@ietcc.csic.es) (M. Frías), [mmonasterio@phi4tech.com](mailto:mmonasterio@phi4tech.com) (M. Monasterio), [rosario.garcia@uam.es](mailto:rosario.garcia@uam.es) (R. García-Giménez), [vigildelavillaraquel@gmail.com](mailto:vigildelavillaraquel@gmail.com) (R. Vigil de la Villa), [malamo@ceisa.es](mailto:malamo@ceisa.es) (M. Álamo).

<https://doi.org/10.1016/j.job.2023.107641>

Received 12 July 2023; Received in revised form 10 August 2023; Accepted 21 August 2023

Available online 22 August 2023

2352-7102/© 2023 The Authors. Published by Elsevier Ltd. This is an open access article under the CC BY license (<http://creativecommons.org/licenses/by/4.0/>).

the last century in Europe.

According to the Intergovernmental Panel on Climate Change, anthropogenic activity is one of the main causes of climate change [6]. Within this context, concrete is the most widely used building material on Earth because of the easy availability of its raw materials, the ability to mold it into any shape or size, its good mechanical properties and durability, and its low cost. The main constituent of concrete is Portland cement, and production of the associated clinker entails the emission of carbon dioxide in both the calcination process and in fuel combustion. Accordingly, the cement sector is the source of about 7.4% of global carbon dioxide emissions [7].

Furthermore, the depletion of natural resources, and the need to preserve them, has driven the introduction of new alternative materials, such as industrial and agricultural waste, industrial by-products, or raw materials available locally in some areas [8,9]. The latter is the case of Cumbre Vieja ash, which may contribute to minimizing carbon dioxide emissions and natural resource use.

Volcanic emissions into the air are normally classified into gases, aerosols, and volcanic ash [10]. Volcanic ash is the main solid emission and consists of rock particles of less than 2 mm in size with an extremely variable diameter. Cumbre Vieja is a volcano located on the island of La Palma (Canary Islands, Spain) that had lain dormant for 50 years before erupting on September 19, 2021, covering a land area spanning 65 km<sup>2</sup> with lava and volcanic ash [1]. The pyroclastic material from the volcanic eruption was ejected as fragments, producing ash fall deposits and scoria cones. In addition, it also spread outwards in ash flow deposits, creating a severe issue for local inhabitants. However, these pyroclastic flows containing a mix of hot lava blocks, pumice, and volcanic ash could be good pozzolanic materials [11–13] suitable for use in the cement industry as a potential Portland cement constituent. Pozzolanic activity is a parameter related to the degree of reaction between a pozzolan (reactive silicon) and calcium hydroxide in the presence of water. This activity can be directly determined by measuring the amount of reacted lime.

Under the principles of the circular economy, these pyroclastic flows have been assessed for potential use in bricks [14,15], geopolymers [16,17], blended cements [11–13], and self-compacting concrete [18,19]. This high-density pyroclastic mix presents a vesicular structure [5,6]. Depending on size, it may either be screened or ground into powder (80 µm [16] or 400 µm mesh [17], respectively). The effect of pozzolanic material fineness on compressive strength has been reported by several authors [20–22]. As expected, the finer the volcanic ash, the higher the pozzolanic activity [23,24]. In contrast, applying a heat treatment to the volcanic ash produced negative results [23].

The effect of incorporating blended cements containing natural pozzolan into mortars and concretes varies according to the nature, fineness, and content of the natural pozzolan, among other parameters. Blended cements have been reported to improve durability [25–31], enhance resistance to sulfate attack [32], increase setting time, reduce water permeability [33], and decrease the heat of hydration [32,34]. With regard to mechanical strength, conflicting results have been found in the literature since this characteristic depends on many factors.

Khan et al. [35] reported that concrete containing up to 15% natural pozzolan as a partial cement replacement matches the performance of concrete containing 20% coal fly ash, which is very close to plain concrete. Furthermore, it has been reported that self-compacting concrete in which a high volume of Portland cement has been replaced with volcanic ash presents good workability, resistance to chloride penetration, and compressive strength properties [19].

Al-Swaidani and Aliyan [36] studied mortar and concrete specimens made with blended cements containing scoria—which consisted of amorphous glassy ground mass, vesicles, plagioclase, and olivine—at replacement levels ranging from 10 to 35%. The 28-day compressive strength of concrete containing scoria was lower than that of the reference concrete, but the chloride resistance of scoria-based concrete was better.

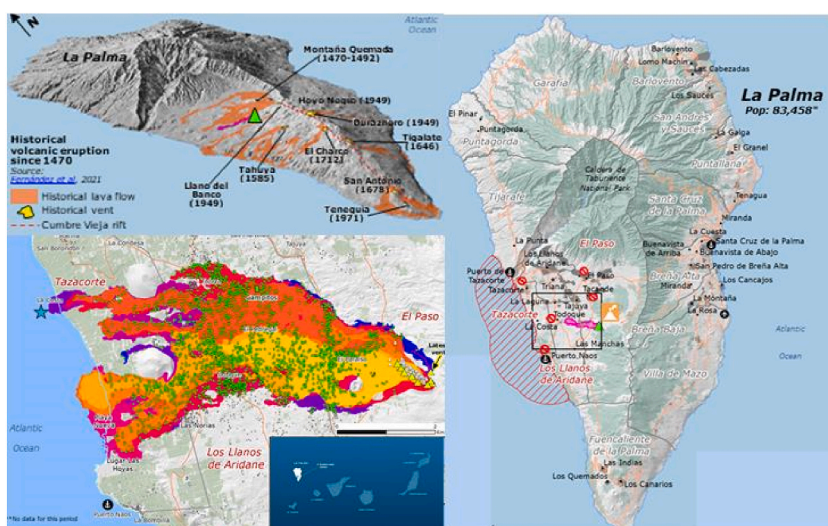


Fig. 1. Location of La Palma within the Canary Islands archipelago and geographical site of the Cumbre Vieja volcano. The red shading indicates the area of the island covered by the lava flows. (For interpretation of the references to color in this figure legend, the reader is referred to the Web version of this article.)

Summing up, utilization of natural pozzolans in the manufacture of blended Portland cements has a significant effect—depending on the replacement ratios and fineness—on the chemical, physical, mechanical, and durability properties of cement-based materials. Furthermore, since natural pozzolans enter the Portland cement production process after calcination they also provide great environmental benefits [37]. The manufacture of one ton of Portland cement clinker requires about 3.6 GJ and releases nearly 825 kg of carbon dioxide into the atmosphere [37]. For this reason, utilization of Cumbre Vieja ash deserves particular attention.

The cement produced in the Canary Islands is almost all CEM II/A-P 42,5 R (241,775 tons in 2021), CEM IV/A (P) (185,323 tons in 2021), and CEM IV/B (P) (131,854 tons in 2021), although most local cement plants also make a low volume of CEM I (15,441 tons in 2021).

In addition to promoting the management and recovery of Cumbre Vieja volcanic ash by the local cement industry, the objective of this research paper is to evaluate the technical and economic feasibility of using Cumbre Vieja volcanic ash as a main constituent in cement production. Consequently, this paper aims to provide a comprehensive study of the use of Cumbre Vieja volcanic ash (in replacement proportions of up to 40%) as a main constituent of cement and its impact on behavior and chemical, physical, and mechanical properties.

## 2. Materials and methods

### 2.1. Raw materials

The island of La Palma has a surface area of 708 km<sup>2</sup>. Although volcanic activity stopped a long time ago in the northern part, it remains active in the southern part of the island. The volcanic eruption on the western slope of Cumbre Vieja occurred in the area known as Hoya de Tajogaite or Cabeza de Vaca. At the time of the eruption, the Tajogaite volcano had an altitude of around 1100 m. The volcanic ash was collected within a reasonable distance of this site. Properties of the volcanic ash change depending on the sampling location, since the cooling rate and temperatures can be slightly different. In any case, the same effect occurs in the well-known coal fly ashes. Depending on the coal power plant, the properties are different [38]. However, all of them can be used as Portland cement constituents due to their high content of the sum of silicon, aluminum and iron oxides of this material. In particular, the high reactive silicon oxide content can be considered as the main parameter to be considered. The collected ash was ground to particle sizes below 45 µm for the characterisation and behavioural studies of the blended cements. It is well-known the effect of the pozzolanic materials fineness on the mechanical strength and durability. For instance, Payá et al. [22] discussed such effect on the mechanical characteristics of coal fly ash; whereas Sanjuán et al. [39] observed this fact on silica fume. Furthermore, Chindaprasirt et al. [40] reported the effect of fly ash fineness on durability.

The Portland cement used in this study (rated CEM I 42.5 R as per European standard EN 197-1:2011 [39]) was provided by the CEISA cement plant in Arguineguín (latitude: 28°07'N, longitude: 15°24'W) on the Canary Islands (Spain), as well as their chemical composition (Table 1).

According to the Bogue formula [40], the potential composition of the cement would be 62.26% C<sub>3</sub>S, 14.70% C<sub>2</sub>S, 6.6% C<sub>3</sub>A, and 10.61% C<sub>4</sub>AF.

The reference cement, CEM I 42.5 R, was partially replaced by volcanic ash (10%, 25%, and 40%). According to European standard EN 197-1, these mix proportions correspond to the CEM II/A-P, CEM II/B-P, and CEM IV/A (P) cements.

The mortars were made with a 1:3 cement/sand ratio and a 0.5 water/binder ratio. German standardized sand (NORMASAND) was also employed. Mixing, molding (4 × 4x16 cm) and curing (under water at 20 °C) were carried out in accordance with the specifications of the standard EN 196-1:2018 [41]. The compressive strengths at 2, 7 and 28 days were tested (average of 6 specimens) using an IBERTESTAUTOTEST 200-10-5 wc press, with a loading speed of 2400 N/s.

### 2.2. Characterization techniques

Chemical analysis of the main oxides was performed by X-ray fluorescence (XRF) using a Bruker S8 Tigger 4 kW device. Loss on ignition (LOI), insoluble residue, and chloride ion were determined as per European standard EN 196-2:2013 [42].

Granulometric distribution analysis was performed on the volcanic ash using a laser diffraction device attached to a Malvern Mastersizer 3000 analyzer (Malvern Panalytical, Madrid, Spain) equipped with red and blue light sources (He-Ne and LED) in dry dispersion mode. The measurement range was 0.01–3500 µm.

The mineralogical composition of the samples was resolved by powder X-ray diffraction (XRD) (Malvern Panalytical, Madrid, Spain) on a PANalytical X'Pert PRO X-ray diffractometer equipped with a Cu anode. Its operating parameters were 40 mA, 45 kV, 0.5 divergence slit, and 0.5 mm slit reception. The samples were scanned with a step size of 0.0167 (2θ) and 150 m s per step. Characterization of the samples was carried out using the random power method, which operates from 5 to 80 (2θ). Measured patterns were qualitatively and quantitatively analyzed using Match v.3 and Fullprof software, respectively, to perform Rietveld analysis. Crystallography Open Database (COD) reference patterns were used to identify the different phases. Table 2 lists the Crystallography Open Database (COD) reference standards used to identify the different phases.

**Table 1**  
Chemical composition by XRF of the Portland cement, CEM I 42.5 R (%).

Constituent	SiO <sub>2</sub>	Al <sub>2</sub> O <sub>3</sub>	Fe <sub>2</sub> O <sub>3</sub>	CaO	MgO	SO <sub>3</sub>	Cl <sup>-</sup>	LOI	IR <sup>a</sup>
CEM I 42.5 R	22.11	5.44	3.12	61.37	1.35	2.92	0.03	1.13	1.89

<sup>a</sup> Insoluble residue measured by the Na<sub>2</sub>CO<sub>3</sub> method (EN 196-2).

Scanning electron microscopy (SEM) and energy-dispersive X-ray spectroscopy (EDX) were used for morphological observation and microanalysis of the samples. The equipment employed comprised an Inspect FEI Electron Microscope (FEI, Hillsboro, OR, USA) equipped with an energy-dispersive X-ray analyzer (W source, DX4i analyzer, and Si/Li detector). The chemical composition presented is the mean value of ten analyses per sample. The results are expressed in oxides (% by weight).

The changes in pore size in the blended mortars were determined by mercury intrusion porosimetry using a Micromeritics Autopore IV porosimeter (Micromeritics, Norcross, GA, USA). The equipment works at pressures of up to 33,000 psi (227.5 MPa) and measures pore diameters between 0.006 and 439  $\mu\text{m}$ .

### 2.3. Methodology

The pozzolanic activity of the ash in the pozzolan/ $\text{Ca}(\text{OH})_2$  system is determined by an accelerated chemical test consisting of adding 1 g of waste to 75 mL of saturated  $\text{Ca}(\text{OH})_2$  solution and keeping the mixture at 40 °C for the duration of the analysis [43]. The proportion of lime fixed by the waste was calculated by comparison with the concentration obtained from a blank test.

The pozzolanic activity of cement mixes containing 25% and 40% volcanic ash was assessed by chemical testing as per the procedure given by European standard EN 196-5:2011 [44]. All the mixes were immersed in a saturated solution of  $\text{Ca}(\text{OH})_2$  at 40 °C for 8 days. The  $\text{CaO}$  and  $\text{OH}^-$  concentrations were then measured at 8 days as per EN 196-2.

The standardized physical characterization tests (water required for normal consistency, setting times, and expansion) and mechanical characterization tests (flexural strength and compression) were performed in accordance with the currently applicable European EN 196-1 and EN 196-3 standards [45,46]. The stress-rupture tests were conducted in an IBERTEST AUTOTEST 200/20-SW press at 2, 7, 28, and 90 days of curing.

The electrical resistivity ( $\rho$ ) of the mortars was measured on  $4 \times 4 \times 16$  cm water-saturated prismatic specimens, starting from demolding and continuing up to 90 days of curing. The Wenner method was used as per Spanish standard UNE 83988-2 [47]. The measurements were performed using a 4-electrode device. The electrodes were placed on the four rectangular faces of the specimens and were spaced 3.5 cm apart. The results reported in this study correspond to the average of the readings taken for each specimen at the hydration time under consideration. The resistivity values obtained ( $\rho$ ) were calculated on the basis of the measurements and according to the Wenner method, applying the following equation:

$$\rho = \rho_w \cdot F_f \quad (1)$$

Where  $F_f$  is the form factor (which is 0.172 for prismatic samples measuring  $4 \times 4 \times 16$ ) and  $\rho_w$  is the Wenner resistivity.

Meanwhile, the form factor ( $q$ ) describes the changes in resistivity over time and is obtained by adjusting the resistivity curve to the time, as per the equation:

$$\rho_t = \rho_0 \left( \frac{t}{t_0} \right)^q \quad (2)$$

Where  $\rho_t$  represents the resistivity at time  $t$  and  $\rho_0$  represents the resistivity at time 0 ( $t_0$ ).

The Fagerlund method, as described in UNE 83982 [48], was used to perform the capillary absorption tests on the selected mortars. For this purpose, after the  $4 \times 4 \times 16$  cm prismatic specimens had been cured for 28 days they were pre-conditioned in several stages as described in Spanish standard UNE 83966 [49]. Once the weight gains had been obtained, the sorptivity coefficients ( $S$ ) were calculated according to Equation (3).

$$\frac{W}{A} = S_0 + S\sqrt{t} \quad (3)$$

Where  $W$  represents the amount of water absorbed,  $A$  is the area of the specimen exposed to water, and  $t$  is time.  $S_0$  is the correction coefficient for the initial amount of water absorbed by the pores.

**Table 2**  
Crystallography Open Database (COD) reference patterns used to identify the different phases.

Phase	Code COD
Olivine	9,000,394
Pyrite	5,000,115
Mackinawite	9,011,800
Goethite $\alpha$	9,016,178
Akaganeite	9,002,990
Maghemite	9,006,316
Ilmenite	1,011,033
Diaspore	1,011,027
Tridymite low	1,250,189
Cristobalite high	1,010,944
Plagioclase	502,990
Mullite	9,010,159
Diopside	1,000,014

### 3. Results and discussion

#### 3.1. Chemical, physical, and mineralogical characterization of volcanic ash

XRF analyses of the volcanic ash (PA) reveal a mostly siliceous nature with  $\text{SiO}_2$  content standing at 45.5% (Fig. 2). It is also important to note the  $\text{Al}_2\text{O}_3$  (14.9%),  $\text{Fe}_2\text{O}_3$  (13.3%),  $\text{CaO}$  (10.8%), and  $\text{MgO}$  (7.0%) content and the negative (−0.5%) LOI, possibly due to the presence of sulfides.

The sum of the silicon, aluminum, and iron oxides amounts to 73.7%, above the minimum required by the US ASTM C618 standard ( $\geq 70\%$ ) [50] for N- and F-type additions and the ash, with a 10.8%  $\text{CaO}$  content, could even present cementing properties. Based on the values shown in Table 1, the blended cements meet the chemical requirements of the currently applicable standards. Table 3 shows the sulfate (expressed as  $\text{SO}_3$ ) and chloride content found in the cements.

As regards physical characterization, the findings of the laser granulometry analysis performed on the ash received are shown in Fig. 3. The analysis reveals uniform granulometry in the 50–800  $\mu\text{m}$  range and maximum distribution density at 224  $\mu\text{m}$ . The D10, D50, and D90 parameter values (diameters by which 10%, 50% and 90% of the particles are lower) are 109, 212, and 424  $\mu\text{m}$ , respectively. Subsequently, the PA was ground to below 45  $\mu\text{m}$  for the experimental part.

Mineralogical analysis of the volcanic ash using XRD (Fig. 4) reveals a large group of ferromagnesian minerals, all exhibiting a low degree of crystallization and high amorphous material content.

The phases present are as follows: olivine  $(\text{Mg, Fe})_2\text{SiO}_4$  (5.10 Å, 3.88 Å, 3.48 Å, 2.76 Å, 2.51 Å and 2.45 Å); pyrite  $\text{FeS}_2$  (3.12 Å, 2.70 Å, 2.42 Å, 2.21 Å, 1.91 Å and 1.63 Å), griegite  $\text{Fe}_3\text{S}_4$  (3.50 Å, 2.98 Å, 2.47 Å, 2.01 Å, 1.90 Å and 1.74 Å), mackinawite  $\text{Fe}_{0.91}\text{Ni}_{0.13}\text{Co}_{0.007}\text{S}$  (5.03 Å, 2.97 Å, 2.31 Å, 1.83 Å, 1.80 Å and 1.72 Å), goethite  $\alpha\text{-FeOOH} - \text{Fe}_2\text{O}_3 \cdot \text{H}_2\text{O}$  (4.18 Å, 2.69 Å, 2.49 Å, 2.45 Å, 2.19 Å and 1.72 Å) akaganeite  $\beta\text{-FeOOH}$  (3.31 Å, 2.54 Å, 2.28 Å, 1.94 Å, 1.74 Å and 1.63 Å), maghemite  $\gamma\text{-Fe}_2\text{O}_3$  (2.95 Å, 2.51 Å, 2.08 Å and 1.60 Å), ilmenite  $\text{FeTiO}_3$  (3.73 Å, 2.75 Å, 2.54 Å, 2.23 Å, 1.86 Å and 1.72 Å), diaspore  $\text{AlOOH}$  (3.99 Å, 2.55 Å, 2.31 Å, 2.13 Å, 2.07 Å and 1.71 Å), tridymite low (4.10 Å, 3.81 Å, 2.97 Å, 2.50 Å and 2.30 Å), cristobalite high (4.15 Å, 2.53 Å, 2.07 Å and 1.64 Å), plagioclases  $\text{NaAlSi}_3\text{O}_8$  to  $\text{CaAl}_2\text{Si}_2\text{O}_8$  (6.4–6.5 Å, 4.03 Å and 3.22–3.16 Å), mullite  $\text{Al}_2\text{O}_3 \cdot \text{SiO}_2$  (3.43 Å, 3.40 Å and 2.21 Å), and diopside  $\text{MgCaSi}_2\text{O}_6$  (4.69 Å, 2.99 Å, 2.89 Å and 2.53 Å).

The mineralogical composition of the volcanic ash sources is a function of the magma generated by the considered volcanic apparatus. The La Palma volcano presents a mineralogy very similar to that of Vesuvius in Italy [51], with olivine, silica group minerals (tridymite, cristobalite, mullite), plagioclases, pyrite, iron and aluminum oxyhydroxides and diopside. This mineralogy is different from that of other volcanic locations such as the Jano volcano in Japan [52] or that of the tephras of Antarctica [53].

The findings of morphological observation of the volcanic ash using SEM are shown in Fig. 5. Its dark color is due to its high iron content. Its vesicular structure is the result of the gases released when the lava was cooling. Its permeability, however, is very low due to the presence of thin, vitreous, intervesicular membranes. The highly rounded iron deposits unevenly cover the surfaces of the aggregates (Table 2).

Material of varying sizes and compositions, and which matches the minerals determined by diffraction (Fig. 6), is deposited on the aggregates.

The varying compositions of the aggregates that provide the growth substratum determine the mineral deposited on their surface. Fig. 7 and Table 4 show, by way of example, formation of sodium or calcium plagioclases dependent on enrichment of these ions in the base aggregate or growth substratum.

Comparing the results of Fig. 2 which analyses the whole volcanic ash and Table 4 which analyses specific zones in each volcanic ash, it is concluded that they are aluminosilicate samples, rich in calcium and ferromagnesian elements, with a low proportion of potash and titanium oxide.

#### 3.2. Pozzolanic activity

##### 3.2.1. Pozzolanic activity in a pozzolan/lime system

The chemical test for pozzolanic activity was performed on the pozzolan/ $\text{Ca}(\text{OH})_2$  system by grinding the La Palma ash (PA) to a fineness of less than 45  $\mu\text{m}$ . The changes in the amount of lime fixed by the PA in relation to reaction time are shown in Fig. 8 together with the values obtained for a fly ash (FA). This solid waste has a siliceous nature coming from a Spanish thermoelectric power plant,

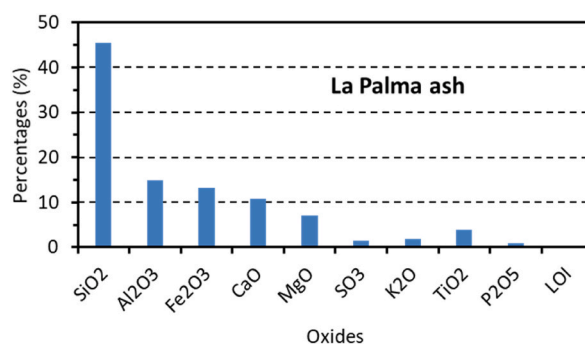


Fig. 2. Chemical composition of La Palma ash as determined by XRF.



**Table 3**  
Standardized chemical requirements for commercial cements.

%	OPC	10% OPC	25% OPC	40% OPC	EN 197-1
SO <sub>3</sub>	2.92	2.73	2.51	2.27	≤3.5–4.0
Cl	0.03	0.03	0.04	0.04	≤0.1

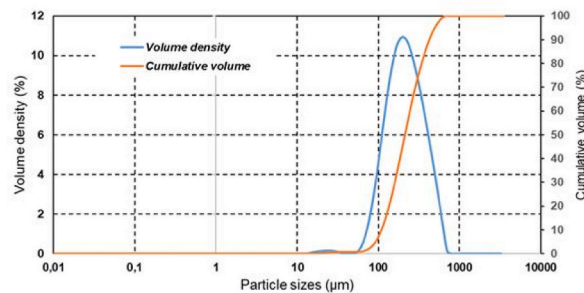


Fig. 3. Granulometric analyses of starting PA as determined by laser granulometry.

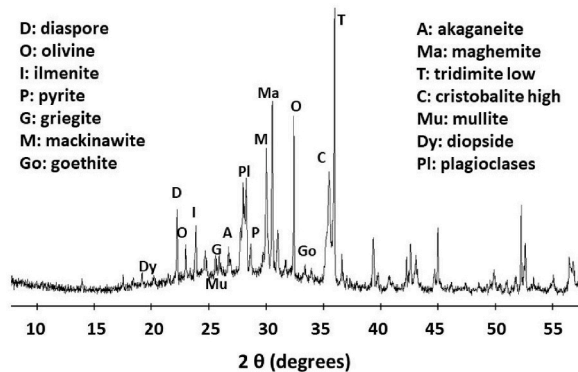


Fig. 4. Mineralogical analysis of PA using XRD.

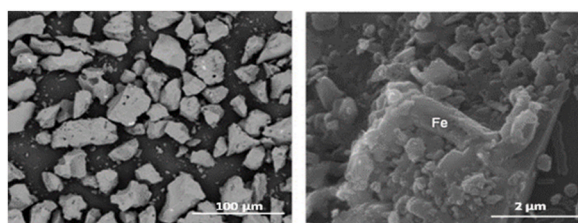


Fig. 5. Morphological analyses of PA. Left: general shape. Right: deposits containing Fe.

which meets the chemical and physical requirements for the manufacture of cements.

The La Palma volcanic ash (PA) shows minimal capacity to react with the lime in the medium over the first 7 days of reaction. From that age onwards, its pozzolanic activity increases considerably, reaching values of 57% and 90% at 28 and 90 days, respectively. This pozzolanic behavior in the pure pozzolan/lime system is similar to that achieved with fly ash produced by thermal power stations. The exception is observed at 28 days of curing, at which point the PA exhibits higher reactivity, by around 13.5%, than the FA.

### 3.2.2. Pozzolanicity method in a pozzolan/cement system

The pozzolanic activity of CEM II/B–P and CEM IV/A (P) cements containing 25% and 40% volcanic ash was assessed as per the procedure described in European standard EN 196-5 [44]. This Frattini method is used to quantify the calcium hydroxide leached from the hydrated Portland cement pastes containing volcanic ash, in aqueous solution, after 8 days. The result for both cements—CEM II/B–P and CEM IV/A (P)—was positive, i.e., the amount of calcium hydroxide in the solution was less than in the saturated concentration (Fig. 9).

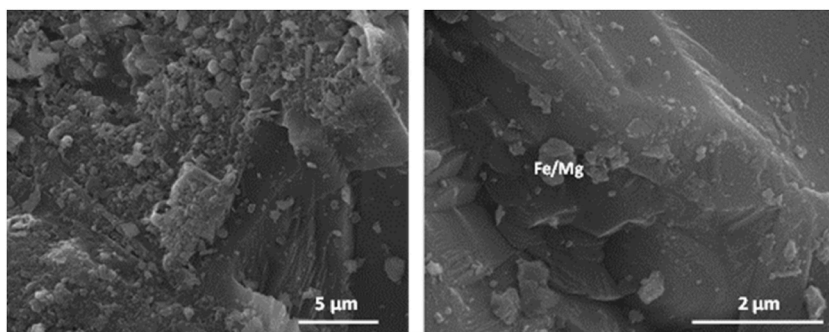


Fig. 6. Left: deposits. Right: olivine formation.

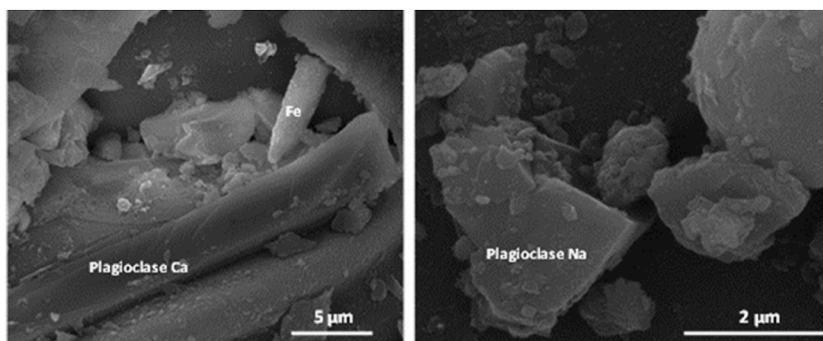


Fig. 7. Left: plagioclase-Ca on Ca substratum. Right: plagioclase Na on Na substratum.

Table 4

Chemical analysis using EDX of aggregates and substratum of volcanic ash (n.d. = not detected).

Oxides (%)	olivine	substratum	deposit with Fe	plagioclase Ca	substratum	plagioclase Na	substratum
Na <sub>2</sub> O	n.d.	3.78	2.52	1.32	6.30	7.06	4.77
MgO	12.16	4.47	1.37	1.75	5.72	1.70	3.94
Al <sub>2</sub> O <sub>3</sub>	4.52	12.35	3.54	24.86	16.19	23.34	13.93
SiO <sub>2</sub>	51.38	40.38	9.78	53.18	48.90	52.34	45.94
K <sub>2</sub> O	n.d.	2.85	n.d.	n.d.	1.96	n.d.	3.21
TiO <sub>2</sub>	n.d.	4.05	n.d.	n.d.	3.24	n.d.	4.07
CaO	5.27	13.32	3.61	15.61	7.79	7.35	10.21
Fe <sub>2</sub> O <sub>3</sub>	26.67	18.8	79.18	3.28	9.90	8.21	13.93

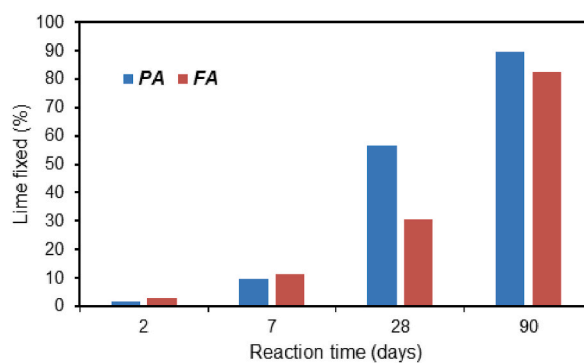


Fig. 8. Changes in the amount of lime fixed in relation to reaction time.

### 3.3. Physical behavior

#### 3.3.1. Physical requirements of cement pastes

Table 5 shows the water required for normal consistency (NCW), initial (IS) and final (FS) setting times, and soundness (S).

Table 5 shows that the difference in setting time between CEM I 42.5 R (OPC) and CEM II/A-P (10% OPC) is minimal. Setting times increase significantly when the ash content is over 10%, reaching a IS delay of around 60 min for replacement percentages between 25 and 40%. This delay could be related to the presence of some chemical elements, in trace contents, such as Ba, Pb, Co [54] and sulphide (pyrite) detected by XRD analysis. The cement pastes made with volcanic ash need more water to achieve normal consistency (NCW), with this amount being 15.8% higher for the 40% OPC paste than for the reference paste. None of the analyzed pastes show variations in volume (S). The analyzed binary cements meet the standardized physical requirements.

#### 3.3.2. Resistivity and capillary absorption in cement mortars

Fig. 10 shows hydration of the mortars as measured by electrical resistivity. The upward trend in the results as hydration time increases indicates greater resistance to the transport of electrical charges over time, which implies a greater number of hydrated phases, at the same time as the matrix of the cement becomes denser [55]. The results show that the OPC mortar reaches 337 Ohm\*m at 90 days of hydration, attaining its highest value at 42 days, after which point the values stabilize. At short hydration times, the mortars containing ash present descending figures that are influenced by the amount of ash added. The lowest values are presented by the mortar containing 40% ash and the highest values by the mortar containing 10%. Both mortars' values are below those of the reference OPC.

From 21 days onwards, however, the slope of the mortar containing 40% ash steepens and from 35 days' hydration onwards the mortar presents the highest resistivity values. Similarly, the mortar containing 25% ash presents the second-highest resistivity from 49 days of hydration onwards. Finally, the sample containing 10% ash exceeds the resistivity values of the reference OPC mortar at 91 days of hydration.

In view of the results, a beneficial effect is observed with the ash incorporation in the cement mortar resistivity since the pozzolanic reaction promotes the secondary C-S-H gel formation, which fill in partially the capillary pores. In addition, the pore solution change enhances mentioned resistivity. This fact is due to the reaction of  $\text{Ca}(\text{OH})_2$  dissolved in the pore solution with the reactive  $\text{SiO}_2$  of ash, among other reactions which remove some ions from the pore solution.

The values in Table 6 show how the age factor increases with the amount of ash added to the mortars, with the value for the 40% OPC mortar being 300% that of the control sample. This tendency would be related to the pozzolanic activity of the volcanic ash, generating denser and more compact matrices. The  $R^2$  values of the 25% and 40% OPC ashes are over 0.98, while in the OPC and 10% OPC mortars they are below 0.90.

These results indicate that adding ash to the mortar matrix accelerates hydration. Activation of the process, however, takes a certain amount of time, which decreases as the amount of ash grows.

The changes in the analyzed mortars' capillary absorption capacity relative to the square root of the time are shown in Fig. 11. The figure shows two distinct behaviors: a very pronounced linear trend for the first 24 h and a second, less steep, linear trend afterwards.

This dual linear behavior is common in mortars and is referred to in ASTM C1585 [56]. This standard indicates two different capillary absorption states (CA), called the first and second sorptivity coefficients, which can be calculated from the slopes observed between 0 and 6 h and between 1 and 7 days, respectively. The results for these slopes and the  $R^2$  values are shown in Table 7.

The  $R^2$  values for both the first and the second absorption are above 0.98 in all the samples except the 40% OPC mortars where the values are slightly lower. Based on the first absorption, the reference OPC mortar shows greatest capacity to absorb water by capillary action, with this coefficient decreasing as the ash content grows. Thus, the mortar with greatest clinker replacement content (40%) presents a coefficient of  $0.0041 \text{ cm/min}^{0.5}$  versus  $0.0070 \text{ cm/min}^{0.5}$  in the OPC mortar, possibly due to the synergy between the filler and pozzolanic effects of the volcanic ash. According to the observations made by Alexander et al. [57], concretes are durable when the sorptivity values are below  $0.14 \text{ cm/min}^{0.5}$ . If this criterion is transferred to the mortars in this study, all the mortars analyzed can be classified as durable.

This reduction in capillary water absorption in the mortars containing volcanic ash is similar to the behavior of FA and blast furnace slag [58] but is different to that of other non-traditional pozzolanic additives such as construction and demolition waste (CDW), whose

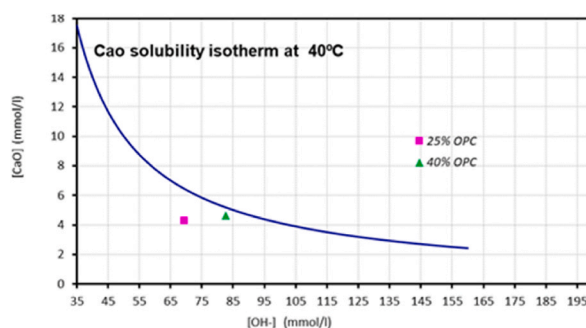


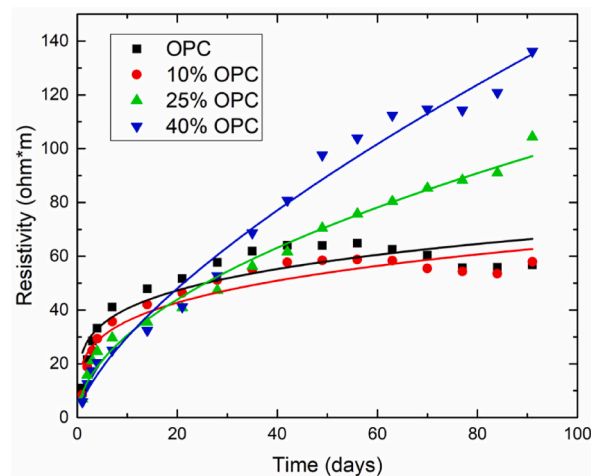
Fig. 9. Pozzolanic test of the binary cements at 8 days.



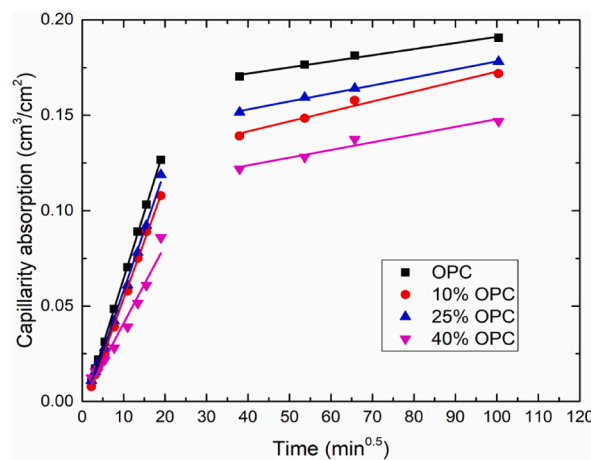
**Table 5**

Water required for normal consistency (NCW), initial (IS) and final (FS) setting times, and soundness (S).

	OPC	10% OPC	25% OPC	40% OPC	EN 197-1
NCW (%)	28.5	29.0	31.5	33.0	–
IS (min)	120	130	220	210	≥45–60
FS (min)	175	195	300	300	–
S (mm)	0.0	0.0	0.0	0.5	≤10

**Fig. 10.** Changes in cement mortar resistivity over the course of the test.**Table 6**Age factor ( $q$ ), resistivity at time 0 ( $\rho_0$ ) and  $R^2$  values.

	OPC	10% OPC	25% OPC	40% OPC
$q$	0.224	0.252	0.524	0.683
$\rho_0$	24.15	20.04	9.13	6.20
$R^2$	0.821	0.889	0.985	0.984

**Fig. 11.** Changes in capillary absorption capacity relative to the square root of the time.

absorption coefficients exceed that of the OPC mortar [59].

### 3.4. Mechanical strength

The compressive strength of the mortars measured at 2, 7, and 28 days is presented in Fig. 12 for the CEM II/A-P, CEM II/B-P, and

**Table 7**  
Capillary absorption coefficients and  $R^2$  values.

Mortar	1st A.S. (cm/min <sup>0.5</sup> )	$R^2$	2nd A.S. (cm/min <sup>0.5</sup> )	$R^2$
OPC	0.0070	0.999	$3.2061 \times 10^{-4}$	0.988
10% OPC	0.0063	0.999	$5.2225 \times 10^{-4}$	0.981
25% OPC	0.0060	0.997	$4.2000 \times 10^{-4}$	0.998
40% OPC	0.0041	0.971	$4.0327 \times 10^{-4}$	0.957

CEM IV/A (P) cements containing 10%, 25%, and 40% volcanic ash, respectively. As shown in Fig. 12, the compressive strength of the mortar specimens at 28 days gradually decreased as the proportion of volcanic ash grew.

Fig. 12 indicates that the difference in compressive strength between CEM I 42.5 R and CEM II/A-P (containing 10% ash) is minimal at 2, 7, and 28 days. The mortars' early strength decreases significantly when the ash content is over 10%. As expected, the ash activity is lower at early ages. Thus, cement hydration is delayed as the ash content increases. CEM IV/A (V), with 40% ash replacement content in the mortars, exhibited worse strength performance than the CEM II/A-V and CEM II/B-V mortars. The 28-day compressive strength is slightly above the lower limit for the 32.5 strength class (37.4 MPa) given by European standard EN 197-1. This suggests that in order to ensure compressive strength performance the upper limit for volcanic ash replacement is about 40%.

Pozzolanicity can also be assessed indirectly by measuring mortars' compressive strength gain when the hydraulic binder (i.e., OPC) is replaced with volcanic ash. This can be determined by the strength activity index (SAI), as described in European standard EN 450-1 [60] or American standard ASTM C311 [61]. The index is defined as the ratio of the compressive strength of a mortar containing 25% (EN 450-1) or 20% (ASTM C311) pozzolanic material to the compressive strength of a mortar made with CEM I cement. The European standard requires a 28-day index greater than or equal to 75% (and 85% at 90 days), whereas the American standard requires an index greater than or equal to 75% at 7 and 28 days.

The SAI at 7 and 28 days is 81.3% and 84.3%, respectively. Accordingly, the 28-day SAI requirement (EN 450-1) is met. Furthermore, it can be estimated that the 7-day SAI requirement (ASTM C311) is also met.

### 3.5. Changes in microporosity in the blended cement mortars

The pore size distribution density curves for the cement mortars made with 10%, 25%, and 40% PA are shown in Fig. 13. All the analyzed mortars present two pore-size zones: a very intense main band located around 100 nm (although porosity is lower in the OPC mortar) that tends toward greater pore size as the added ash content increases, and a second band of lesser intensity below 50 nm, indicating a process of refinement of the pore network as the ash content increases. The greatest pore refinement is seen in the OPC mortars with 25% and 40% replacement content.

The final synergistic result of these two effects (greater and lesser refinement according to ash content) produces greater total porosity the higher the volcanic ash content, as shown in Table 8.

These total porosity values are in line, on the one hand, with the decrease in compressive strength discussed above and, on the other, with the behavior of mortars containing fly ash [62] and other industrial waste [63].

## 4. Conclusions

The eruption at the Cumbre Vieja volcanic ridge (La Palma, Canary Islands, Spain), which lasted for 85 days between September and December 2021, was the strongest and longest-lasting eruption on record on the island. The emission of ash had a far-reaching impact since it covered settlements and farmland. At the time, this event attracted global attention. In this paper, we have focused on the potential use of this material as a main Portland cement constituent. Accordingly, the following conclusions may be drawn from this study:

1. The ash from the recent volcanic eruption on the island of La Palma (Canary Islands, Spain) is mainly siliceous in nature ( $\text{SiO}_2 = 45\%$ ) and contains calcium oxides, alumina, and iron in concentrations ranging between 10% and 15%. The sum of the acid oxides

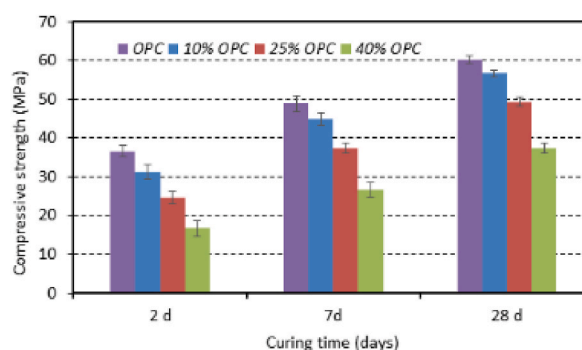


**Fig. 12.** Compressive strength at 2, 7, and 28 days for CEM II/A-P, CEM II/B-P, and CEM IV/A (P) cements containing 10%, 25%, and 40% volcanic ash.

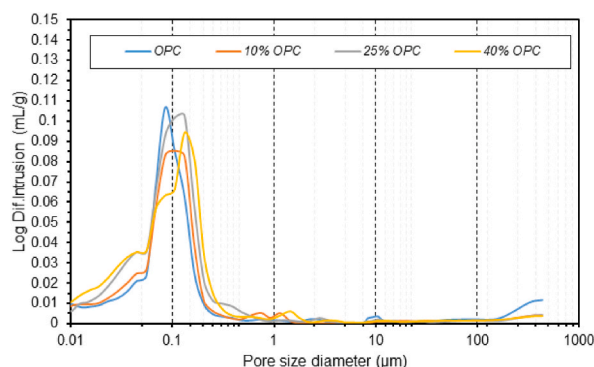


Fig. 13. Pore size density curves for mortars at 28 days of curing.

Table 8

Total porosity values for the analyzed mortars.

Porosity	OPC	10% OPC	25% OPC	40% OPC
%	11.71	12.85	14.02	14.41

exceeds 70%, meaning the ash can be considered a material with pozzolanic properties. The binary cements meet the standardized chemical requirements for sulfate and chloride content.

- Mineralogically, the ash mostly consists of tridymite, olivine, maghemite, diaspore, ilmenite, pyrite, and mackinawite phases.
- From a pozzolanic point of view, the volcanic ash possesses a high capacity to fix the lime in the medium at 90 days of reaction in the pozzolan/lime system, comparable to the capacity found in fly ash. The cement paste tests using the standardized Frattini method show that the 25% and 40% cement pastes meet the pozzolanicity test criteria at 8 days.
- The analyzed binary cements meet the standardized physical requirements for initial setting time and soundness. A delay in both setting times is observed in samples with up to 25% replacement content and there is a greater quantity of water when fly ash is added to produce a consistency comparable to that of the reference paste.
- The resistivity values obtained show that the mortars with 25% and 40% replacement content present very high age factor ( $q$ ) values versus their OPC and 10% OPC counterparts, mainly due to the synergy between the filler and pozzolanic effects.
- The first capillary absorption coefficients show a marked decrease as volcanic ash content increases, dropping from  $0.0070 \text{ cm/min}^{0.5}$  in the OPC mortar to  $0.0041 \text{ cm/min}^{0.5}$  in the 40% OPC mortar. Based on the maximum absorption value set for concretes ( $<0.14 \text{ cm/min}^{0.5}$ ), the analyzed mortars would be classified as durable.
- At all ages, the compressive strength of the mortars decreases as volcanic ash is added. The mortar with 40% replacement content would be one strength category lower than the reference mortar.
- Adding volcanic ash to the cement matrix produces an increase in total porosity, reaching a value 23.06% higher in the 40% OPC than in the reference OPC. For pore sizes below  $50 \mu\text{m}$ , however, the behavior is the opposite.

In light of the findings of this research paper, the scientific and technical feasibility of using PA as a secondary raw material in cement manufacture is evident (CEM II/A-P, CEM II/B-P, and CEM IV/A-P with a lower clinker content and lower carbon footprint). Furthermore, it paves the way for future research focusing principally on aspects relating to medium- and long-term durability and strength.

#### Author statement

This work has not been financed by any funding

#### Declaration of competing interest

The authors declare that they have no known competing financial interests or personal relationships that could have appeared to influence the work reported in this paper.

#### Data availability

Data will be made available on request.

#### Acknowledgments

The authors gratefully acknowledge Cementos Especiales de las Islas, S.A. (CEISA) for providing the volcanic ash.

## References

- [1] M.A. Longpré, A. Felpeto, Historical volcanism in the Canary Islands; part 1: a review of precursory and eruptive activity, eruption parameter estimates, and implications for hazard assessment, *J. Volcanol. Geoth. Res.* 419 (2021), 107363, <https://doi.org/10.1016/j.jvolgeores.2021.107363>.
- [2] J. Fernández, J. Escayo, Z. Hu, A.G. Camacho, S.V. Samsonov, J.F. Prieto, K.F. Tiampo, M. Palano, J.J. Mallorqui, E. Ancochea, Detection of volcanic unrest onset in La Palma, Canary Islands, evolution and implications, *Sci. Rep.* 11 (2021) 1–15, <https://doi.org/10.1038/s41598-021-82292-3>.
- [3] <https://ignesp.maps.arcgis.com/>. (Accessed 27 January 2023).
- [4] P.A. Paez, M.G. Cogliati, A.T. Caselli, M. A. A.M. Monasterio, An analysis of volcanic SO<sub>2</sub> and ash emissions from Copahue volcano, *J. S. Am. Earth Sci.* 110 (2021), 103365, <https://doi.org/10.1016/j.jsames.2021.103365>.
- [5] A.E. Bedoya-Velásquez, M. Hoyos-Restrepo, A. Barreto, R.D. García, P.M. Romero-Campos, O. García, R. Ramos, R. Roininen, C. Toledano, M. Sicard, R. Ceoloto, Estimation of the mass concentration of volcanic ash using ceilometers: study of fresh and transported plumes from La Palma volcano, *Rem. Sens.* 14 (2022) 5680, <https://doi.org/10.3390/rs14225680>.
- [6] IPCC, Summary for policymakers, in: P.R. Shukla, J. Skea, R. Slade, A. Al Khouradajie, R. van Diemen, D. McCollum, M. Pathak, S. Some, P. Vyas, R. Fradera, M. Belkacemi, A. Hasija, G. Lisboa, S. Luz, J. Malley (Eds.), *Climate Change 2022: Mitigation of Climate Change. Contribution of Working Group III to the Sixth Assessment Report of the Intergovernmental Panel on Climate Change*, Cambridge University Press, Cambridge, UK and New York, NY, USA, 2022, <https://doi.org/10.1017/9781009157926.001>.
- [7] M.A. Sanjuán, C. Andrade, P. Mora, A. Zaragoza, Carbon dioxide uptake by cement-based materials: a Spanish case study, *Appl. Sci.* 10 (2020), <https://doi.org/10.3390/app10010339>.
- [8] S. Hammat, B. Menadi, S. Kenai, C. Thomas, M.S. Kirgiz, A.G. de Sousa, The effect of content and fineness of natural pozzolana on the rheological, mechanical, and durability properties of self-compacting mortar, *J. Build. Eng.* 44 (2021), 103276, <https://doi.org/10.1016/j.jobbe.2021.103276>.
- [9] L.H. Pereira, F. Briol, J.R. Tamashiro, A. Kinoshita, Potential of bamboo leaf ash as supplementary binder materials – a systematic literature review, *J. Build. Eng.* 71 (2023), 106547, <https://doi.org/10.1016/j.jobbe.2023.106547>.
- [10] C. Stewart, D.E. Damby, J. Claire, H. Tamar Elias, E. Ilyinskaya, I. Tomašek, B.M. Longo, A. Schmidt, H. Krage Carlsen, E.y Mason, P.J. Baxter, S. Cronin, C. Witham, Volcanic air pollution and human health: recent advances and future directions, *Bull. Volcanol.* 84 (2022), <https://doi.org/10.1007/s00445-021-01513-9>.
- [11] J. Rosales, M. Rosales, J.L. Díaz-López, F. Agrela, M. Cabrera, Effect of processed volcanic ash as active mineral addition for cement manufacture, *Materials* 15 (2022) 6305, <https://doi.org/10.3390/ma15186305>.
- [12] J.J. Santana, N. Rodríguez-Brito, C. Blanco-Peñalver, V.F. Mena, R.M. Souto, Durability of reinforced concrete with additions of natural pozzolans of volcanic origin, *Materials* 15 (2022) 8352, <https://doi.org/10.3390/ma15238352>.
- [13] M.M. Tashima, L. Soriano, M.V. Borrachero, J. Monzó, J. Payá, Towards the valorization of Cumbre Vieja volcanic ash – production of alternative cements, *Construct. Build. Mater.* 370 (2023), 130635, <https://doi.org/10.1016/j.conbuildmat.2023.130635>.
- [14] P. Zhang, J. Huang, Z. Shen, X. Wang, F. Luo, P. Zhang, J. Wang, S. Miao, Fired hollow clay bricks manufactured from black cotton soils and natural pozzolans in Kenya, *Construct. Build. Mater.* 141 (2017) 435–441, <https://doi.org/10.1016/j.conbuildmat.2017.03.018>.
- [15] G. Cultrone, The use of Mount Etna volcanic ash in the production of bricks with good physical-mechanical performance: converting a problematic waste product into a resource for the construction industry, *Ceram. Int.* 48 (2022) 5724–5736, <https://doi.org/10.1016/j.ceramint.2021.11.119>.
- [16] H. Tchakoute, A. Elimbi, E. Yanne, C. Djangang, Utilization of volcanic ashes for the production of geopolymers cured at ambient temperature, *Cem. Concr. Compos.* 38 (2013) 75–81, <https://doi.org/10.1016/j.cemconcomp.2013.03.010>.
- [17] P.N. Lemounga, K.J. MacKenzie, U.C. Melo, Synthesis and thermal properties of inorganic polymers (geopolymers) for structural and refractory applications from volcanic ash, *Ceram. Int.* 37 (2011) 3011–3018, <https://doi.org/10.1016/j.ceramint.2011.05.002>.
- [18] N. Abdulmalek, J. Chakkamalayath, Cost-benefit analysis of vibrated cement concrete and self-compacting concrete containing recycled aggregates and natural pozzolana, *J. Eng. Res.* (2022), <https://doi.org/10.36909/jer.15999> epub ahead of print.
- [19] K. Celik, M.D. Jackson, M. Mancio, C. Meral, A.H. Emwas, P.K. Mehta, P.J. Monteiro, High-volume natural volcanic pozzolan and limestone powder as partial replacements for portland cement in self-compacting and sustainable concrete, *Cem. Concr. Compos.* 45 (2014) 136–147, <https://doi.org/10.1016/j.cemconcomp.2013.09.003>.
- [20] E. Alemayehu, B. Lennartz, Virgin volcanic rocks: kinetics and equilibrium studies for the adsorption of cadmium from water, *J. Hazard Mater.* 169 (2009) 395–401, <https://doi.org/10.1016/j.jhazmat.2009.03.109>.
- [21] M.A. Sanjuán, C. Argiz, Fineness of coal fly ash for use in cement and concrete, *Fuel* 2 (2021) 471–486, <https://doi.org/10.3390/fuels2040027>.
- [22] J. Payá, J.M. Monzó, M. Borrachero, E. Peris-Mora, F. Amahjour, Mechanical treatment of fly ashes: Part IV. Strength development of ground fly ash-cement mortars cured at different temperatures, *Cement Concr. Res.* 30 (2000) 543–551, [https://doi.org/10.1016/S0008-8846\(00\)00218-0](https://doi.org/10.1016/S0008-8846(00)00218-0).
- [23] K. Khan, M.N. Amin, M. Usman, M. Imran, M.A. Al-Faiad, F.I. Shalabi, Effect of fineness and heat treatment on the pozzolanic activity of natural volcanic ash for its utilization as supplementary cementitious materials, *Crystals* 12 (2022) 302, <https://doi.org/10.3390/cryst12020302>.
- [24] G.M.S. Abdullah, I.M.H. Alshaikh, A.M. Zeyad, H.M. Magbool, B.H.A. Bakar, The effect of openings on the performance of self-compacting concrete with volcanic pumice powder and different steel fibers, *Case Stud. Constr. Mater.* 17 (2022), e01148, <https://doi.org/10.1016/j.cscm.2022.e01148>.
- [25] C. Dedeloudis, M. Zervaki, K. Sideris, M. Juenger, N. Alderete, S. Kamali-Bernard, Y. Villagrán, R. Snellings, Natural pozzolans. RILEM state-art rep, in: N. De Belie, et al. (Eds.), *Properties of Fresh and Hardened Concrete Containing Supplementary Cementitious Materials*, RILEM State-Of-The-Art Reports 25, vol. 25, 2018, pp. 181–231, [https://doi.org/10.1007/978-3-319-70606-1\\_6](https://doi.org/10.1007/978-3-319-70606-1_6).
- [26] M. Frías, J. Cabrera, The Effect of temperature on the hydration rate and stability of the hydration phases of Metakaolin–Lime–Water systems, *Cement Concr. Res.* 32 (2002) 133–138, [https://doi.org/10.1016/S0008-8846\(01\)00642-1](https://doi.org/10.1016/S0008-8846(01)00642-1).
- [27] J. Xia, Q. Guan, Y. Zhou, J. Wang, C. Gao, Y. He, Z. Wang, P. Song, Use of natural pozzolans in high-performance concrete for the Mombasa–Nairobi railway, *Adv. Cement Res.* 33 (2021) 318–330, <https://doi.org/10.1680/jadcr.20.00045>.
- [28] A.R.L. Kushnir, M.J. Heap, L. Griffiths, F.B. Wadsworth, A. Langella, P. Baud, T. Reuschlé, J.E. Kendrick, J.E.P. Utle, The fire resistance of high-strength concrete containing natural zeolites, *Cem. Concr. Compos.* 116 (2021), 103897, <https://doi.org/10.1016/j.cemconcomp.2020.103897>.
- [29] O. Hunyak, K. Sobol, T. Markiv, V. Bidos, The effect of natural pozzolans on properties of vibropressed interlocking concrete blocks in different curing conditions, *Prod. Eng. Arch.* 22 (2019) 3–6, <https://doi.org/10.30657/pea.2019.22.01>.
- [30] A. Çavdar, S. Yetgin, Availability of tuffs from Northeast of Turkey as natural pozzolan on cement, some chemical and mechanical relationships, *Construct. Build. Mater.* 21 (2007) 2066–2071, <https://doi.org/10.1016/j.conbuildmat.2006.05.034>.
- [31] T. Markiv, K. Sobol, M. Franas, W. Franas, Mechanical and durability properties of concretes incorporating natural zeolite, *Arch. Civ. Mech. Eng.* 16 (2016) 554–562, <https://doi.org/10.1016/j.acme.2016.03.013>.
- [32] M. Najimi, M. Jamshidi, A. Pourkhorshidi, Durability of concretes containing natural pozzolan, *Proc. Inst. Civ. Eng. Constr. Mater.* 161 (2008) 113–118, <https://doi.org/10.1680/coma.2008.161.3.113>.
- [33] B. Ahmadi, M. Shekarchi, Use of natural zeolite as a supplementary cementitious material, *Cem. Concr. Compos.* 32 (2010) 134–141, <https://doi.org/10.1016/j.cemconcomp.2009.10.006>.
- [34] M.I. Sánchez de Rojas, M. Frías, J. Rivera, Studies about the heat of hydration developed in mortars with natural and by-product materials, *Mater. Construcción* 260 (2000) 39–48, <https://materconstrucc.revistas.csic.es/index.php/materconstrucc/article/view/389>.
- [35] M. Khan, A. Alhozaimey, Properties of natural pozzolan and its potential utilization in environmental friendly concrete, *Can. J. Civ. Eng.* 38 (2011) 71–78, <https://doi.org/10.1139/L10-112>.
- [36] A.M. Al-Swaidani, S.D. Aliyan, Effect of adding scoria as cement replacement on durability-related properties, *Int. J. Concr. Struct. Mater.* 9 (2015) 241–254, <https://doi.org/10.1007/s40069-015-0101-z>.

- [37] M.A. Sanjuán, C. Argiz, P. Mora, A. Zaragoza, Carbon dioxide uptake in the roadmap 2050 of the Spanish cement industry, *Energies* 13 (2020) 3452, <https://doi.org/10.3390/en13133452>.
- [38] C. Argiz, E. Menéndez, A. Moragues, M.A. Sanjuán, Fly ash characteristics of Spanish coal-fired power plants, *Afinidad* 72 (2015) 269–277, <http://www.raco.cat/index.php/afinidad/article/viewFile/305569/395407>.
- [39] M.A. Sanjuán, C. Argiz, J.C. Gálvez, A. Moragues, Effect of silica fume fineness on the improvement of Portland cement strength performance, *Construct. Build. Mater.* 96 (2015) 55–64, <https://doi.org/10.1016/j.conbuildmat.2015.07.092>.
- [40] P. Chindaprasit, S. Homwuttiwong, V. Sirivivatnanon, Influence of fly ash fineness on strength, drying shrinkage and sulfate resistance of blended cement mortar, *Cement Concr. Res.* 34 (2004) 1087–1092, <https://doi.org/10.1016/j.cemconres.2003.11.021>.
- [41] European standard EN 197-1, *Cement – Part 1: Composition, Specifications and Conformity Criteria for Common Cements*, 2011.
- [42] Spanish standard UNE 80304 *Cements, Calculations of Potential Composition of Portland Clinker*, 2010.
- [43] European standard EN 196-1, *Methods of Testing Cement - Part 1: Determination of Strength*, 2016.
- [44] European standard EN 196-2, *Methods of Testing Cement - Part 2: Chemical Analysis of the Cement*, 2014.
- [45] M. Frías, R. García, R. Vigil, S. Ferreira, Calcination of art paper sludge waste for the use as a supplementary cementing material, *Appl. Clay Sci.* 42 (2008) 189–193, <https://doi.org/10.1016/j.clay.2008.01.013>.
- [46] European standard EN 196-5, *Methods of Testing Cement – Part 5: Pozzolanicity Test for Pozzolan Cement*, 2011.
- [47] European standard EN 196-1, *Methods of Testing Cement – Part 1: Determination of Strength*, 2018.
- [48] European standard EN 196-3, *Methods of Testing Cement - Part 3: Determination of Setting Times and Soundness*, 2017.
- [49] Spanish standard UNE 83988-2, *Durabilidad del hormigón. Métodos de ensayo. Determinación de la resistividad eléctrica. Parte 2, Método de las cuatro puntas o de Wenner*, 2014.
- [50] Spanish standard UNE 83982, *Durabilidad del hormigón. Métodos de ensayo. Determinación de la absorción de agua por capilaridad del hormigón endurecido, Método Fagerlund*, 2008.
- [51] Spanish standard UNE 83966, *Durabilidad del hormigón. Métodos de ensayo. Acondicionamiento de probetas de hormigón para los ensayos de permeabilidad a gases y capilaridad*, 2008.
- [52] American standard ASTM C618–15, *Standard Specification for Coal Fly Ash and Raw or Calcined Natural Pozzolan for Use in Concrete*, 2015.
- [53] I. Etxebarria, M. Veneranda, I. Costantini, N. Prieto-Taboada, A. Larranaga, C. Marieta, B. de Nigris, A. Martellone, V. Amoretti, G. Arana, J.M. Madariaga, K. Castro, Testing the volcanic material burying Pompeii as pozzolan component for compatible conservation mortars, *Case Stud. Constr. Mater.* 18 (2023), 02194, <https://doi.org/10.1016/j.cscm.2023.e02194>.
- [54] K. Marumoto, Y. Sudo, Y. Nagamatsu, Collateral variations between the concentrations of mercury and other water soluble ions in volcanic ash samples and volcanic activity during the 2014–2016 eruptive episodes at Aso volcano, Japan, *J. Volcanol. Geoth. Res.* 341 (2017) 149–157, <https://doi.org/10.1016/j.jvolgeores.2017.05.022>.
- [55] C.J. Harpel, P.R. Kyle, N.W. Dunbar, Englacial tephrstratigraphy of Erebus volcano, Antarctica, *J. Volcanol. Geoth. Res.* 177 (2008) 549–568, <https://doi.org/10.1016/j.jvolgeores.2008.06.001>.
- [56] A. Rodríguez, R. Días, M. Zumbado, M.M. Bernal, A. Acosta, A. Macías, M.M. Travieso, C. Rial, L.A. Henríquez, L.D. Boada, O.P. Luzardo, Impact of chemical elements released by the volcanic eruption of La Palma (Canary Islands, Spain) on banana agriculture and European consumers, *Chemosphere* 293 (2022), 133508, <https://doi.org/10.1016/j.chemosphere.2021.133508>.
- [57] W.J. McCarter, T.M. Chrisp, G. Starrs, A. Adamson, P.A.M. Basheer, S.V. Namukuttan, S. Srinivasan, C. Green, Characterization of physio-chemical processes and hydration kinetics in concretes containing supplementary cementitious materials using electrical property measurements, *Cement Concr. Res.* 50 (2013) 26–33, <https://doi.org/10.1016/j.cemconres.2013.03.008>.
- [58] American standard ASTM C1585, *Standard Test Method for Measurement of Rate of Absorption of Water by Hydraulic Cement Concretes*, 2020.
- [59] M.G. Alexander, Y. Ballim, K. Stanish, A framework for use of durability indexes in performance-based design and specifications for reinforced concrete structures, *Mater. Struct. Constr.* 41 (2008) 921–936, <https://doi.org/10.1617/s11527-007-9295-0>.
- [60] O. Karanhan, Transport properties of high volume fly ash or slag concrete exposed to high temperature, *Construct. Build. Mater.* 152 (2017) 898–906, <https://doi.org/10.1016/j.conbuildmat.2017.07.051>.
- [61] M. Monasterio, L. Caneda, I. Vegas, M. Frías, Progress in the influence of recycled construction and demolition mineral-based blends on the physical-mechanical behaviour of ternary cementitious matrices, *Construct. Build. Mater.* 344 (2022), 128169, <https://doi.org/10.1016/j.conbuildmat.2022.128169>.
- [62] European Standard EN 450-1, *Fly Ash for Concrete - Part 1: Definition, specifications and conformity criteria*, 2013.
- [63] American standard C311/C311M, *Standard Test Methods for Sampling and Testing Fly Ash or Natural Pozzolans for Use in Portland-Cement Concrete*, 2022.